

The Teddy-Tool v1.1: temporal disaggregation of daily climate model data for climate impact analysis

Florian Zabel¹, Benjamin Poschlod²

¹Ludwig-Maximilians-Universität München (LMU), Department of Geography, Luisenstr. 37, 80333 Munich, Germany

²Research Unit Sustainability and Climate Risks, Center for Earth System Research and Sustainability, Universität Hamburg, Grindelberg 5, 20144 Hamburg, Germany

Correspondence to: Florian Zabel (f.zabel@lmu.de)

Abstract

Climate models provide required input data for global or regional climate impact analysis in temporally aggregated form, often in daily resolution to save space on data servers. Today, many impact models work with daily data, however, sub-daily climate information is getting increasingly important for more and more models from different sectors, such as the agricultural, the water, and the energy sector. Therefore, the open source Teddy-Tool (**temporal disaggregation of daily climate model data**) has been developed to disaggregate (temporally downscale) daily climate data to sub-daily hourly values. Here, we describe and validate the temporal disaggregation, which is based on the choice of daily climate analogues. In this study, we apply the Teddy-Tool to disaggregate bias-corrected climate model data from the Coupled Model Intercomparison Project Phase 6 (CMIP6). We choose to disaggregate temperature, precipitation, humidity, longwave radiation, shortwave radiation, surface pressure, and wind speed. As a reference, globally available bias-corrected hourly reanalysis WFDE5 data from 1980-2019 are used to take specific local and seasonal features of the empirical diurnal profiles into account. For a given location and day within the climate model data, the Teddy-Tool screens the reference data set to find the most similar meteorological day based on rank statistics. The diurnal profile of the reference data is then applied on the climate model. The physical dependency between variables is preserved, since the diurnal profile of all variables is taken from the same, most similar meteorological day of the historical reanalysis dataset. Mass and energy are strictly preserved by the Teddy-Tool to exactly reproduce the daily values from the climate models.

For evaluation, we aggregate the hourly WFDE5 data to daily values and apply the Teddy-Tool for disaggregation. Thereby, we compare the original hourly data with the data disaggregated by Teddy. We perform a sensitivity analysis of different time window sizes used for finding the most similar meteorological day in the past. In addition, we perform a cross-validation and autocorrelation analysis for 30 globally distributed samples around the world, representing different climate zones. The validation shows that Teddy is able to reproduce historical diurnal courses with high correlations >0.9 for all variables, except for wind speed (>0.75) and precipitation (>0.5). We discuss limitations of the method regarding the reproduction of precipitation extremes, inter-day connectivity, and disaggregation of end-of-century projections with strong warming. Depending on the use case, sub-daily data provided by the Teddy-Tool could make climate impact assessments more robust and reliable.

1. Introduction

41 Sub-daily climate data is becoming increasingly important in climate impact analysis. This type of data,
42 which captures variations in temperature, precipitation, and other weather variables at intervals of
43 less than a day, can provide a more detailed representation of local and regional climate conditions
44 and temporal variations. This information can be crucial for evaluating the impacts of climate change
45 on various sectors, such as agriculture, water resources, energy production, and human health (Golub
46 et al., 2022; Trinanes and Martinez-Urtaza, 2021; Colón-González et al., 2021; Tittensor et al., 2021;
47 Byers et al., 2018; Jägermeyr et al., 2021; Poschlod and Ludwig, 2021; Degife et al., 2021). A better
48 representation of the diurnal course of temperature, extreme precipitation events, and other weather
49 variables are also important for adaptation assessments which depend on behavior or processes with
50 high temporal dynamics, such as the energy demand, labor activity, the heat stress of crops or flood
51 events (Minoli et al., 2022; Zabel et al., 2021; Reed et al., 2022; Orlov et al., 2021; Franke et al., 2022;
52 Poschlod 2022). Research has shown that using sub-daily climate data can result in more robust and
53 reliable impact assessments compared to using daily data (Orlov et al. 2023).

54 Today, most climate model data are available for download at daily resolution because of the high
55 storage requirements for sub-daily climate data (Juckes et al., 2020). However, the demand for sub-
56 daily data is increasing with future developments of data management expected to handle this
57 demand with decreasing costs for storage and computing resources (Lüttgau & Kunkel, 2018). Different
58 methods exist to disaggregate available daily climate data to sub-daily, most often hourly values. These
59 can be roughly divided into statistical methods, weather generators, and mechanistic approaches,
60 although mixed forms also exist (Förster et al., 2016).

61 Mechanistic methods use regional climate models to dynamically downscale atmospheric conditions
62 in time and space, usually for a limited area (Vormoor and Skaugen, 2013; Liu et al., 2011; Kunstmann
63 and Stadler, 2005). Weather generators generate synthetic sequences of hourly weather variables by
64 using random number generators that match statistics (Ailliot et al., 2015; Mezghani and Hingray,
65 2009). Various statistical methods exist for temporal disaggregation of daily climate data, ranging from
66 simple interpolations or deterministic approaches to non-parametric approaches and methods that
67 derive statistical relationships from historical data or look for climate analogues (Bennett et al., 2020;
68 Breinl and Di Baldassarre, 2019; Chen, 2016; Debele et al., 2007; Förster et al., 2016; Görner et al.,
69 2021; Liston and Elder, 2006; Park and Chung, 2020; Verfaillie et al., 2017; Poschlod et al., 2018; Zhao
70 et al., 2021). Each of these methods has its own advantages and limitations, and the choice of method
71 depends on factors such as the specific needs of the impact assessment, the quality of the available
72 data, and computational resources.

73 Here, we introduce the Teddy-Tool (**temporal disaggregation of daily climate model data**), which uses
74 statistical methods for temporal disaggregation of daily climate model data. Existing statistical
75 approaches are often only valid for a specific location and cannot be applied globally. In addition,
76 available disaggregation tools often focus on only one variable (e.g. Pui et al., 2012) and therefore do
77 not consider physical interdependencies between different variables, such as precipitation, humidity,
78 temperature, and radiation. Teddy has been specifically developed as a globally applicable tool for
79 climate impact studies. For this purpose, Teddy strictly preserves mass and energy of daily climate
80 model data for each variable throughout the disaggregation procedure. Teddy additionally aims at
81 taking regional and seasonal climate characteristics into account and considers the physical
82 consistency between variables.

83 Teddy represents an easy-to-use tool that can be applied for climate impact assessments in different
 84 sectors that allows a physically consistent temporal disaggregation of daily climate model data. The
 85 Teddy-Tool has been written in Matlab and is available open source via Zenodo (see code availability).

86 2. Data and data requirements

87 In principal, the Teddy-Tool can be used with any climate input, but has specifically been developed to
 88 be used with daily climate data for historical time periods and future scenarios from the Inter-Sectoral
 89 Impact Model Intercomparison Project (ISIMIP). which ISIMIP offers a framework for consistently
 90 projecting the impacts of climate change across affected sectors and spatial scales (Warszawski et al.,
 91 2014). To guarantee cross-sectoral consistency in ISIMIP, all sectors are provided with the same climate
 92 data. ISIMIP provides bias-corrected climate model data from the Coupled Model Intercomparison
 93 Project Phase 6 (CMIP6) and trend-preserving reanalysis climate data (Lange, 2019). Within ISIMIP,
 94 some modeling communities from different sectors have expressed their need for sub-daily climate
 95 data, including the agricultural and the energy sector.

96 Daily bias-corrected climate model data are provided by ISIMIP at 0.5° spatial resolution for air
 97 temperature (tas), humidity (hurs), shortwave radiation (rsds), longwave radiation (rls), air pressure
 98 (ps), wind speed (sfcwind), and precipitation (pr) (Lange, 2019). For air temperature, the daily
 99 maximum (tasmax) and minimum (tasmin) values are additionally provided. ISIMIP provides CMIP6
 100 data for the climate models GFDL-ESM4, IPSL-CM6A-LR, MPI-ESM1-2-HR, MRI-ESM2-0, and UKESM1-
 101 0-LL.

102 Teddy requires hourly climate data as a reference for temporal disaggregation. Therefore, we use the
 103 WFDE5 dataset, which has been generated using the WATCH Forcing Data (WFD) methodology applied
 104 to ERA5 reanalysis data (Cucchi et al., 2020). The bias-adjusted hourly WFDE5 data is globally available
 105 for the time period between 1979 and 2019 at 0.5° spatial resolution. It is consistent with the bias-
 106 adjustment procedure within ISIMIP (Lange, 2019) and thus provides a consistent hourly reference
 107 data for Teddy.

108 Table 1 gives an overview of the available variables and the required datasets at their temporal
 109 resolution. The temporal resolution of the Teddy output is adjustable by the user and can be set to 1-
 110 , 2-, 3-, 4-, 6-, 8-, or 12-hourly values.

111 Table 1: Variables and units of used hourly (h) and daily (d) climate data and the Teddy output. For
 112 WFDE5, the specific variable name is provided in brackets. WFDE5 variables have instantaneous values,
 113 while SWdown, LWdown, Rainf and Snowf have average values over the next hour at each time step.

Variable	WFDE5 (h)	ISIMIP Climate Model (d)	Teddy (flexible)
tas	K (Tair)	K	K
tasmin	-	K	-
tasmax	-	K	-
hurs/huss	kg/kg (Qair)	%	%
rsds	W m ⁻² (SWdown)	W m ⁻²	W m ⁻²

rlds	$W m^{-2}$ (LWdown)	$W m^{-2}$	$W m^{-2}$
pr	$kg m^{-2} s^{-1}$ (Rainf+Snowf)	$kg m^{-2} s^{-1}$	mm timestep ⁻¹
ps	Pa (PSurf)	Pa	hPa
sfcwind	$m s^{-1}$ (Wind)	$m s^{-1}$	$m s^{-1}$

114

115 3. Methods

116 Teddy uses an empirical approach, which 1) selects the ‘most similar meteorological day’ for the daily
 117 climate model data (here: ISIMIP CMIP6 data) within the reference climate data (here: WFDE5) at the
 118 same location. 2) Teddy applies the location-specific diurnal course to each variable of the daily climate
 119 model data for a day of interest. In the following, the procedure is explained in detail, where the
 120 example case of ISIMIP climate data and WFDE5 reference data is used for further illustration:

121 In a first precalculation step, in order to minimize computational resources, hourly WFDE5 data are
 122 aggregated to daily values and stored as NetCDF files. The daily aggregation uses mean values for all
 123 variables and daily sums for precipitation. In addition, rainfall and snowfall fluxes must be summed up
 124 for WFDE5. Daily maximum and minimum temperature are calculated from the hourly data. Units of
 125 climate inputs are converted to match the Teddy output (see Tab. 1). For the conversion of specific
 126 humidity to relative humidity, the Buck equation is applied (Buck, 1981).

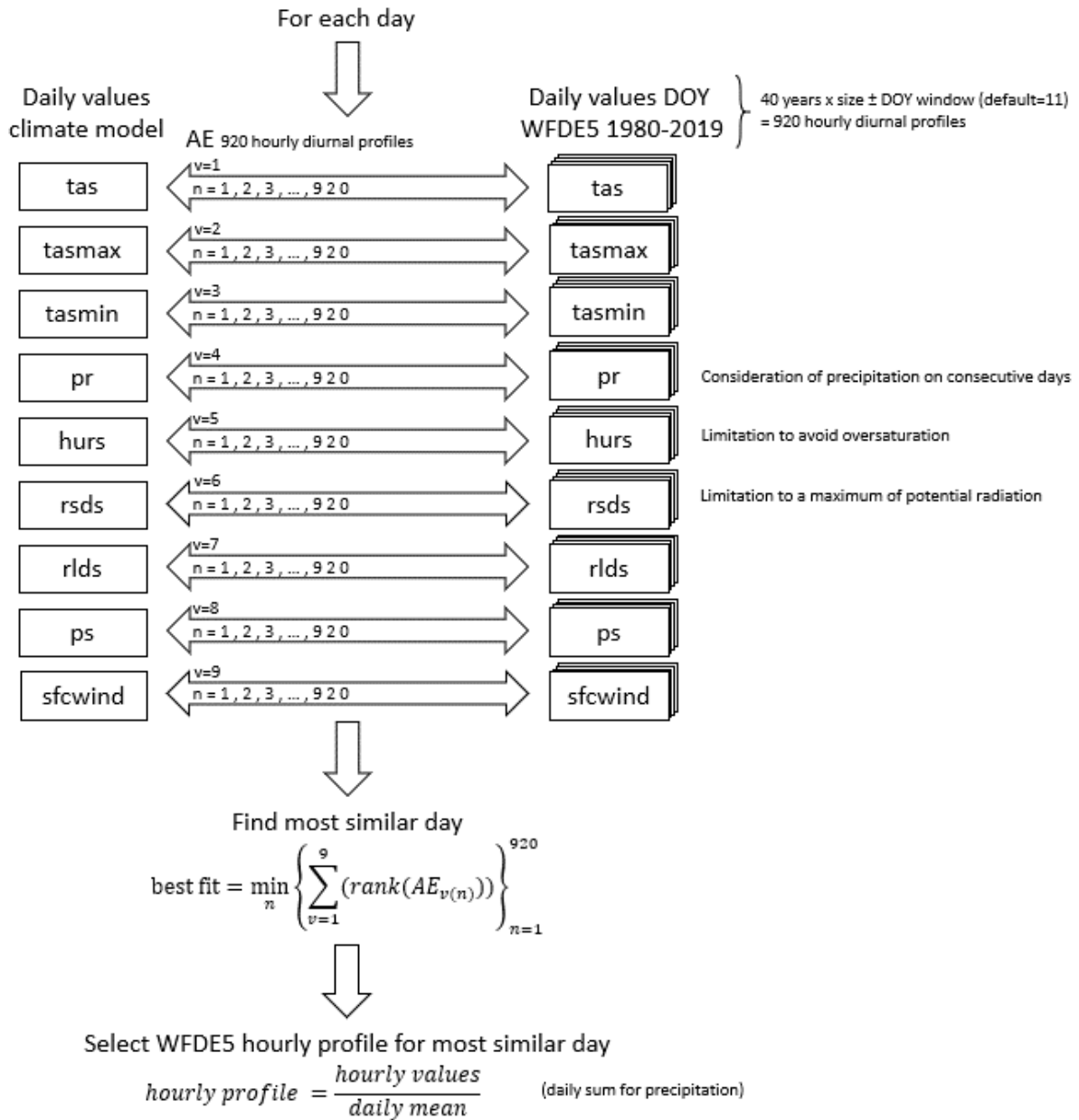
127 After reading the daily climate model data for the selected location (latitude/longitude) that
 128 determines a specific grid cell at 0.5° resolution, the daily mean values of all ISIMIP variables (see Tab.
 129 1) are compared to the aggregated daily values of WFDE5 for a specific time step in order to identify
 130 the most similar meteorological day. For the comparison, a day-of-year (DOY) window can be selected
 131 by the user that allows for a selection of days around the DOY of the actual time step. By default, the
 132 DOY window size is set to 11, which means a sequence of ± 11 days around the actual DOY. As a result,
 133 23 days are selected from each of the 40 WFDE5 reference years (1980-2019). These 920 days now
 134 serve as the statistical population for further calculations (Fig. 1). In a next step, the climate model day
 135 of interest and the statistical population of 920 WFDE5 days are classified according to their
 136 precipitation state (wet / dry). As climate models tend to produce too many days with low-intensity
 137 precipitation called ‘drizzle bias’ (Chen et al., 2021), days with aggregated daily precipitation values
 138 below 1 mm per day are considered as dry days (Sun et al., 2006). Depending on the precipitation state
 139 of the previous day, the day of interest and the following day, there are eight classes: dry-dry-dry, dry-
 140 dry-wet, wet-dry-dry, wet-dry-wet, dry-wet-dry, dry-wet-wet, wet-wet-dry, and wet-wet-wet. This
 141 step is included to better reproduce the inter-day connectivity of precipitation (Li et al., 2018). Only
 142 days with the same precipitation class as the climate model day of interest are selected for the further
 143 course. Next, the absolute error (AE) between daily climate model and aggregated daily WFDE5 data
 144 for each variable is calculated for the remaining statistical population and ranked in ascending order.
 145 The ranking approach is chosen, since the absolute or relative errors of different meteorological
 146 variables cannot be compared to each other. The ranks are cumulated with equal weight over all
 147 variables for each day of the statistical population. In this context, we define ‘the most similar
 148 meteorological day’ as the day with the minimum sum of ranks (Fig. 1). Thus, the ‘most similar
 149 meteorological day’ refers to the statistical similarity of all available daily near-surface meteorological
 150 variables at a given location and time. The approach works under the assumption that similar daily

151 values would have a similar sub-daily profile (Li et al., 2018; Pui et al., 2012; Sharma et al., 2006).
152 Finally, the hourly values are taken from the most similar meteorological day of the WFDE5 reference
153 dataset for each variable and are divided by the WFDE5 daily mean (sum for precipitation) value of the
154 selected day, in order to refer to relative diurnal profiles without absolute variations (Fig. 1). The hourly
155 profile is then applied for each variable to the daily mean (sum for precipitation) value from the climate
156 model. Thus, the daily mean value (sum for precipitation) of the climate model is conserved and
157 reproduced by the disaggregated values.

158 For temperature, the resulting hourly temperature is further scaled between the provided minimum
159 and maximum. The scaling is performed in a way that the daily mean value is preserved with an
160 accuracy of four decimals. Relative humidity is limited to 100%, considering the preservation of the
161 daily mean value.

162 Large selected DOY windows increase the statistical population, but on the other sight might distort
163 climatic characteristics with a strong seasonal course such as shortwave radiation values for the actual
164 DOY. Therefore, we preprocessed hourly potential (cloud free) solar radiation for each DOY globally at
165 0.5° spatial resolution. This data is used as upper bound to limit the resulting hourly values for the
166 corresponding DOY, while the daily mean value is preserved.

167 In a final step, the hourly values are aggregated to the temporal resolution as set by the user.



168

169 Figure 1: Procedure to identify the most similar meteorological day in the population of WFDE5
 170 reference data for the default DOY window of ± 11 days around the actual DOY.

171 In rare cases, precipitation cannot be distributed, due to no precipitation in the reference data. This
 172 can happen in dry deserts, where 40 years of WFDE5 data show no precipitation record within the
 173 range of the moving DOY window (Supplementary Fig. S1 shows a map where this is the case). To
 174 handle this exception, several options are implemented. First, the DOY window is automatically
 175 expanded to $+50$ days around the actual DOY in order to increase the statistical population and thus
 176 the probability to include a precipitation event. If still no precipitation event is found in the reference,
 177 a linear regression between the precipitation amount and the precipitation duration is performed for
 178 the specific location across the entire available data spectrum. The linear regression determines the
 179 usual duration of the selected precipitation event. Subsequently, an hour is randomly selected for the
 180 start of the precipitation event. A goal of Teddy was to consider the physical consistency of inter-
 181 variable relationships. Precipitation generally affects other climate variables (e.g. humidity, radiation,
 182 temperature, etc.; Meredith et al., 2021). During night, physical interdependencies between

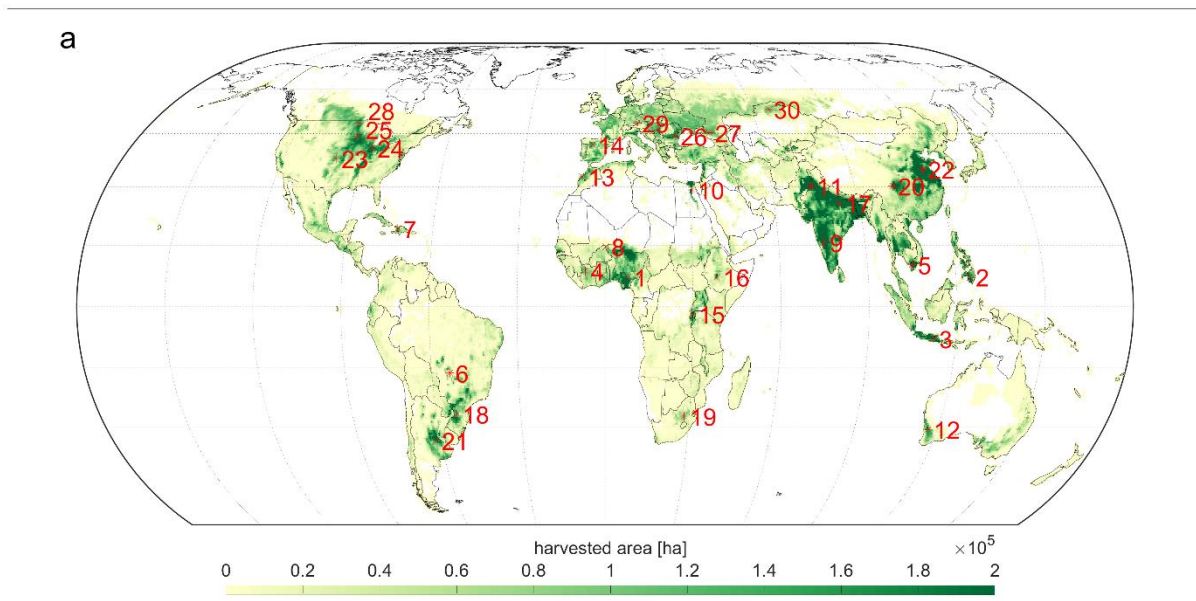
183 precipitation and other variables are generally lower, because radiation is not affected and less energy
184 is available to affect other variables. This might have an effect for impact models, because, as an
185 example, evapotranspiration might be unrealistically high if precipitation occurs at the same time with
186 full solar irradiation during noon. In order to reduce possible inconsistencies with other variables that
187 could lead to implications in impact models, the precipitation is only distributed to hours at nighttime.
188 Alternatively, we implemented the option for the user to write Not a Number (NaN) values instead.

189 Drizzle precipitation (values below 1 mm day⁻¹) is also disaggregated to sub-daily values in order to
190 ensure mass and energy conservation. If no historical precipitation event is found for this case,
191 precipitation noise is again randomly distributed to an hour at nighttime. If no hour without radiation
192 occurs (e.g. high latitudes in northern summer), the precipitation is distributed to local midnight.

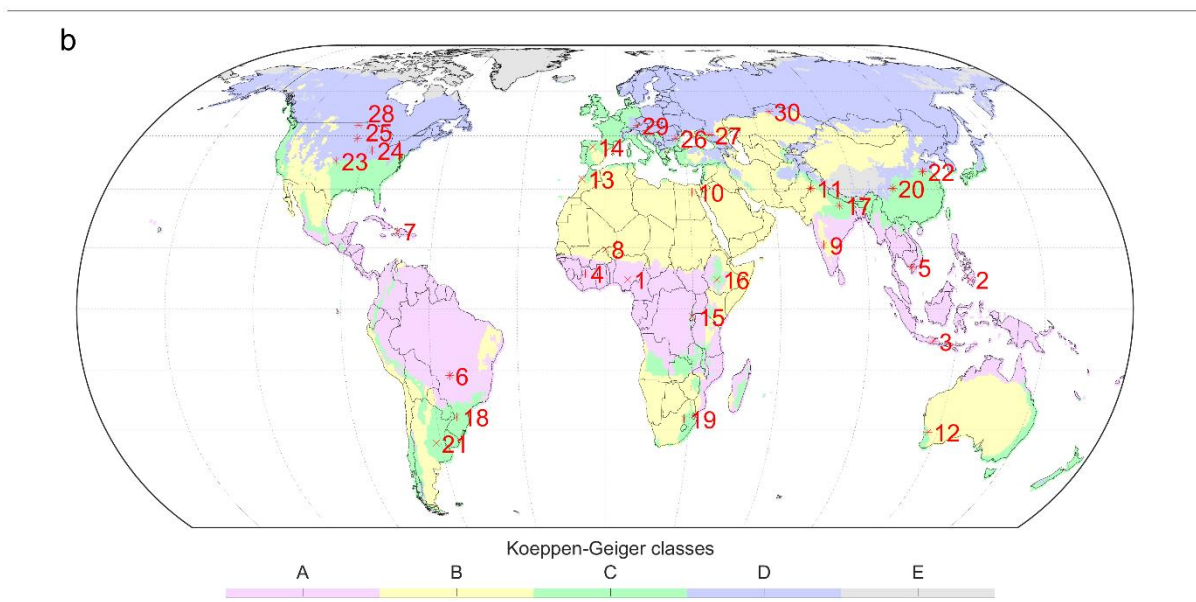
193 The calculation procedure can be performed either for universal time (UT) or for local solar time (LST).
194 The latter divides the world into equal time zones of 15° with the central time zone (+/-7.5°) at
195 Greenwich.

196 **4. Results**

197 In a first step, Teddy is applied for 30 globally distributed samples (Fig. 2) for the year 2010. To be able
198 to validate the results, we perform a cross-validation. Therefore, WFDE5 data for 2010 aggregated to
199 daily values serve as an input for Teddy. The same year is excluded from the statistical population
200 during the cross-validation. As a result, it can be tested how well WFDE5 hourly values for the year
201 2010 are reproduced with the statistical population of the other 39 years. The 30 samples are chosen
202 to represent globally relevant agricultural production regions in different climate zones (Fig. 2). To
203 evaluate the sensitivity of the different DOY window sizes, we run the cross-validation with different
204 DOY window sizes, ranging from 1 to 25, in steps of two, including the option to disable the DOY
205 window (DOY window size = 0). In order to additionally validate the performance for extreme events,
206 we perform a second cross-validation for all available 40 years (1980-2019) with DOY window sizes of
207 11 for sample location 29, located in Southern Germany.



208

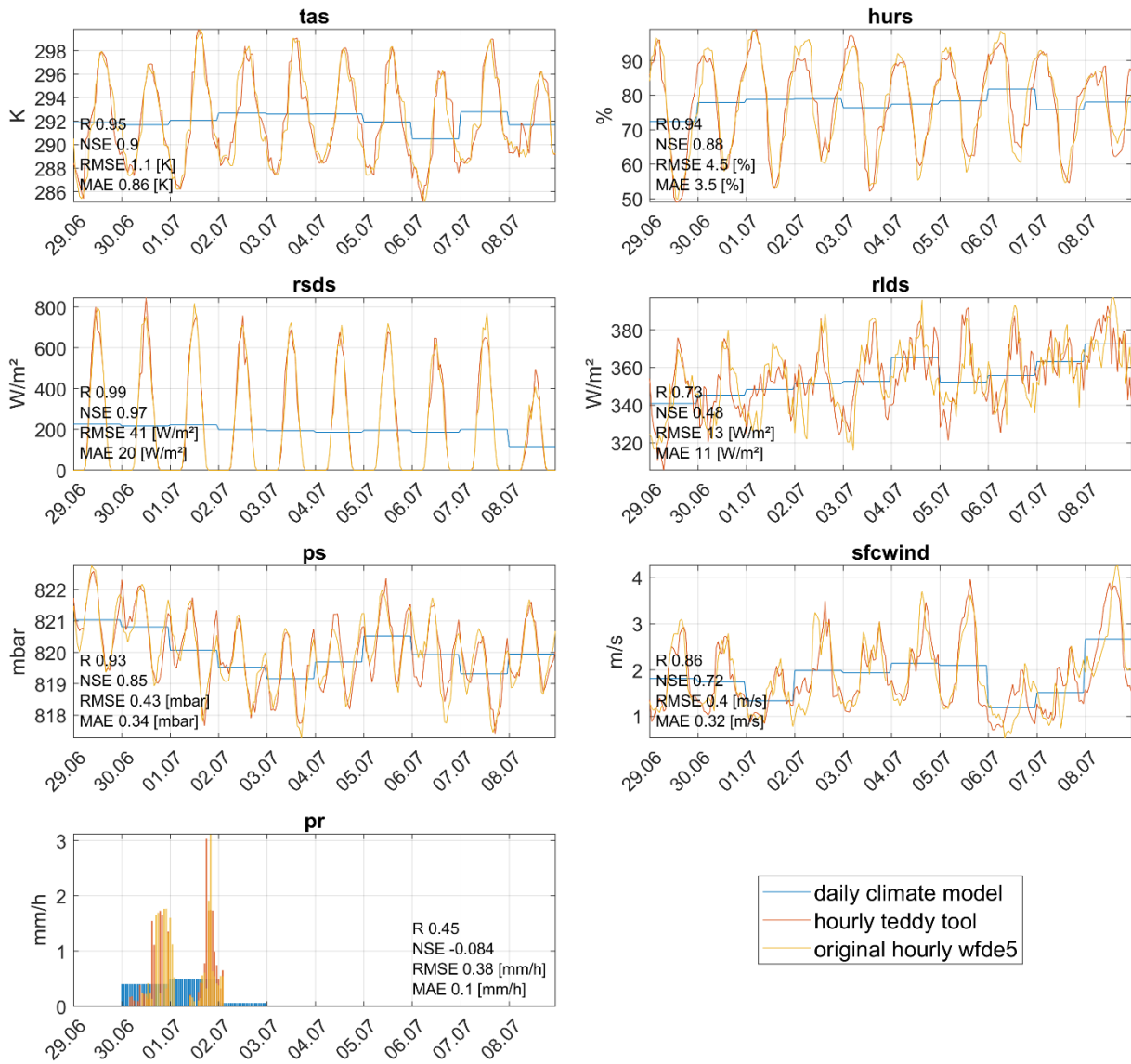


209

210 Figure 2: Distribution of 30 global samples used for the cross-validation on (a) annual total harvested
 211 area of rainfed and irrigated crops in hectare per pixel at a 30 arc-minute grid (Portmann et al., 2010)
 212 and (b) for Koeppen-Geiger climate zones calculated for 1980-2019 WFDE5 temperature and
 213 precipitation values (Beck et al., 2018). Samples are ordered by climate zone affiliation and their
 214 distance to the equator.

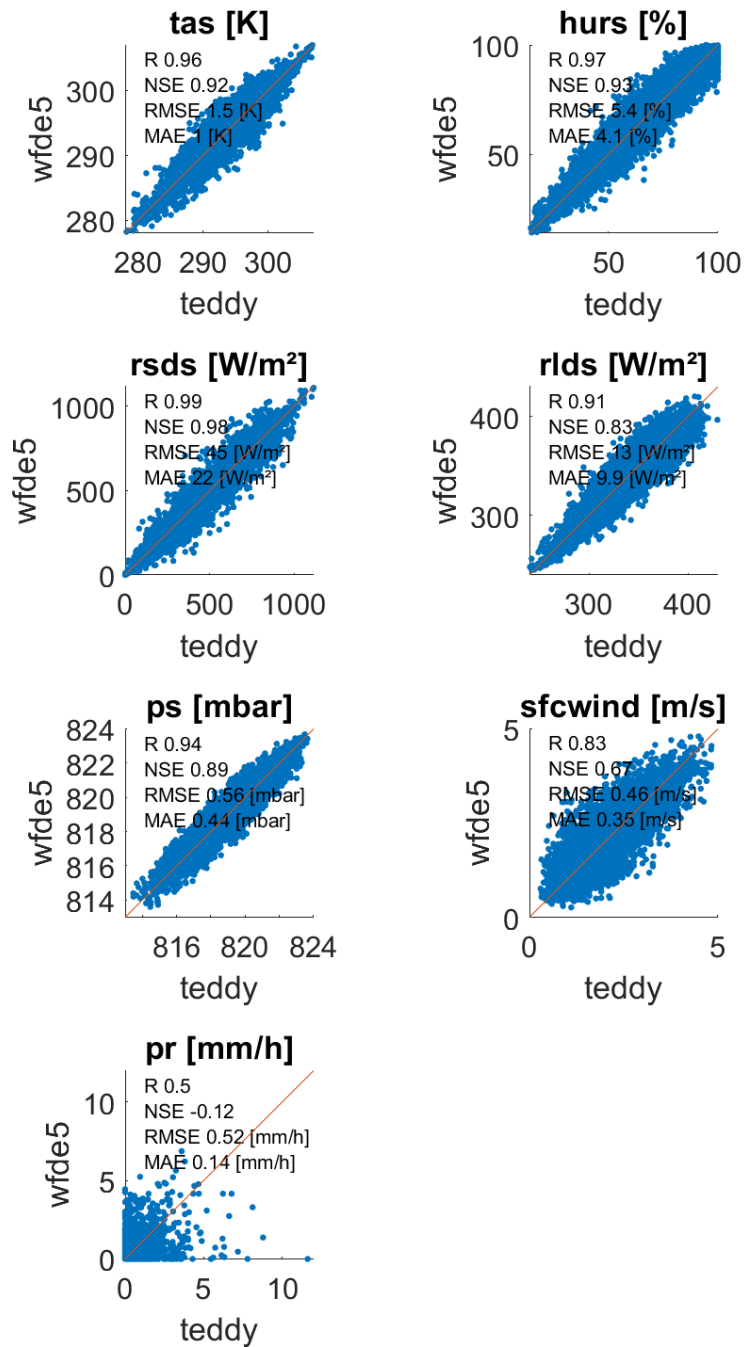
215 4.1 Validation

216 As an example, for sample location 16 in Ethiopia, Fig. 3 shows the results of the temporal
 217 disaggregation series for the cross-validation for a 10-day time series in 2010 in comparison with the
 218 daily climate input and the original hourly WFDE5 data. The hourly courses show high correlations for
 219 the randomly selected time series for all variables except for precipitation (Fig. 3 and scatterplots in
 220 Fig. 4 for the entire year; Supplementary Fig. S2 and S3 alternatively show sample location 22 in China).



221

222 Figure 3: Time-series for all variables comparing daily climate model data, disaggregated hourly results
 223 of Teddy from the performed cross-validation and the original hourly WFDE5 data, shown for sample
 224 location 16 in Ethiopia with a DOY window size of 7 for the 10-day period 29.06. – 08.07.2010. The
 225 Pearson correlation coefficient (R), the Nash-Sutcliffe model efficiency coefficient (NSE), the root mean
 226 squared error (RMSE) and the mean absolute error (MAE) are displayed for the shown time period for
 227 each variable.



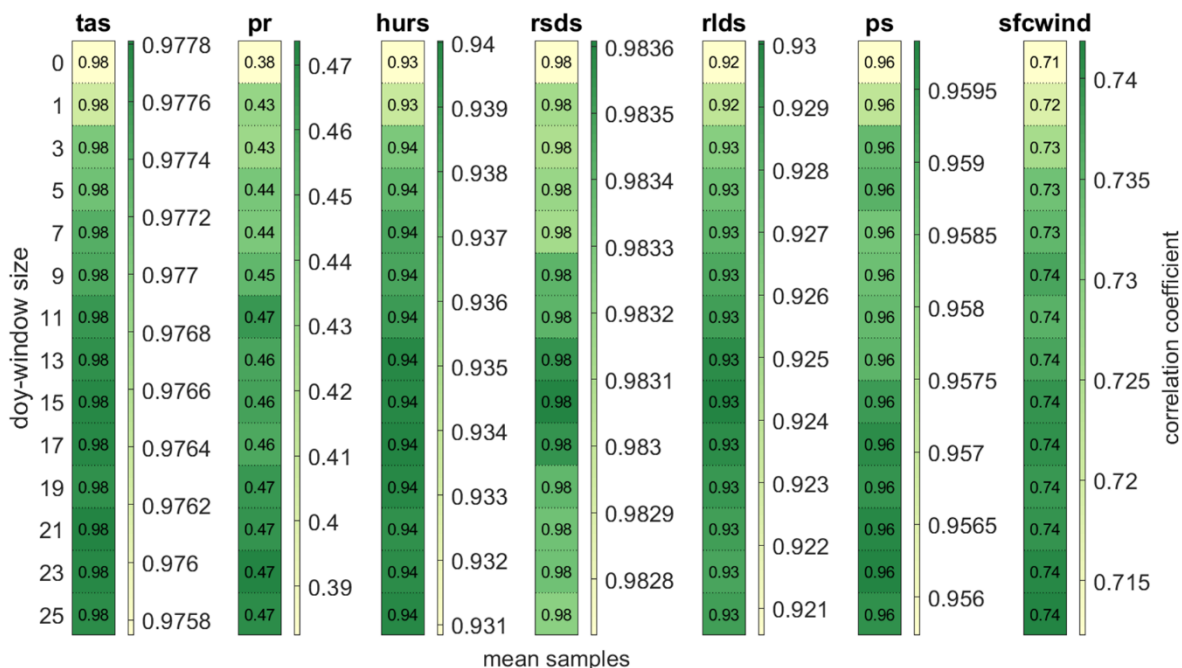
228

229 Figure 4: Hourly values for the year 2010 between disaggregated values generated by the Teddy-Tool
 230 and the original WFDE5 data used for the cross-validation, exemplarily for sample location 16 in
 231 Ethiopia with a DOY window size of 7. The Pearson correlation coefficient (R), the Nash-Sutcliffe model
 232 efficiency coefficient (NSE), the root mean squared error (RMSE) and the mean absolute error (MAE)
 233 are displayed for each variable.

234 4.2 Sensitivity analysis DOY window size

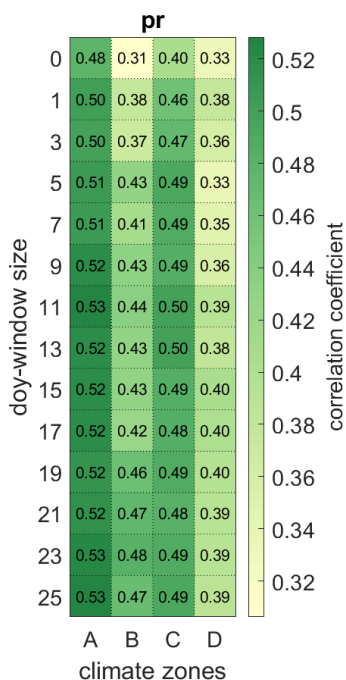
235 The sensitivity analysis averaged over all 30 samples shows that the Pearson correlation coefficient of
 236 hourly values for the year 2010 show high correlations for all variables ($r > 0.9$), except wind speed
 237 ($r > 0.7$) and precipitation ($r > 0.4$), which are generally more difficult to disaggregate (Fig. 5;
 238 Supplementary Fig. S4 additionally shows the Nash-Sutcliffe model efficiency coefficient). The selected
 239 DOY window size has an effect on the quality of the results. While no DOY window (size=0) results in

240 the lowest correlation coefficient across all variables, the DOY window size does significantly affect the
 241 correlation for precipitation and wind speed (Fig. 5).



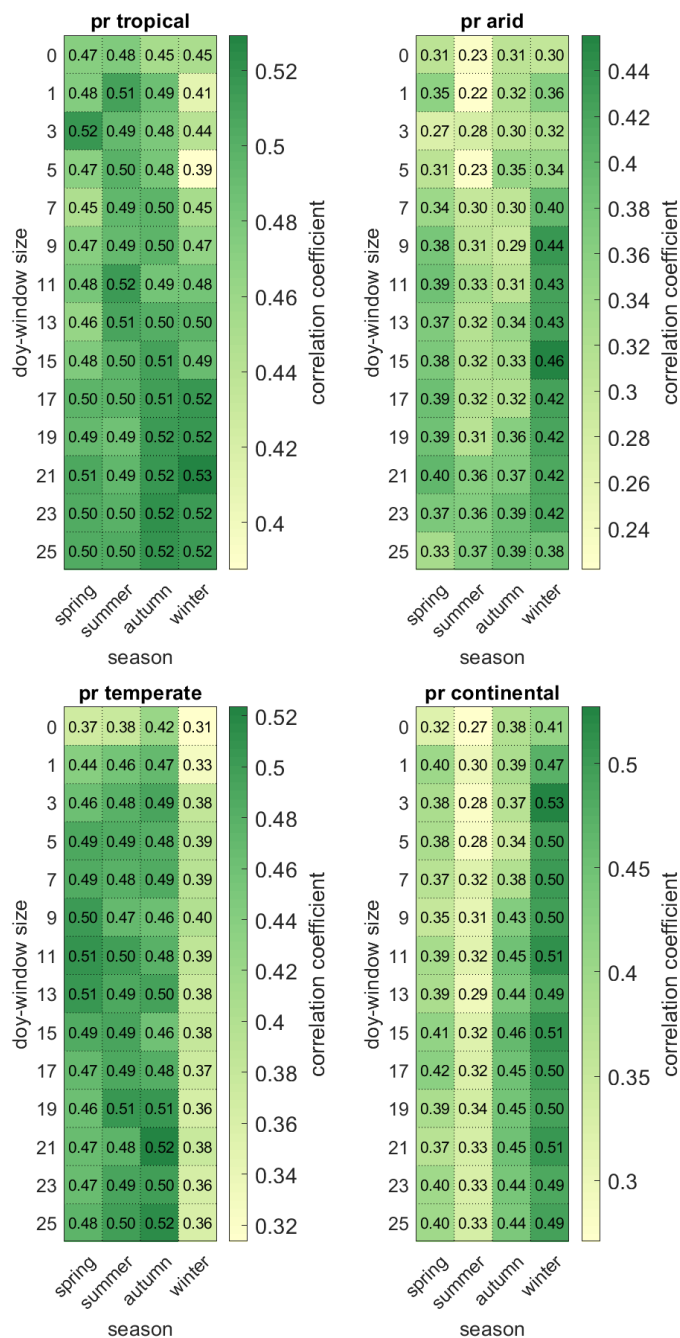
242
 243 Figure 5: Pearson correlation coefficient for different DOY window sizes averaged over all 30 samples
 244 for the year 2010 for all variables being disaggregated to hourly values. The scaling of the colorbar
 245 differs between variables.

246 For precipitation, the impact of the DOY window size on the correlation varies between regions. Larger
 247 DOY windows are mainly beneficial for precipitation in arid regions, while showing lower increases in
 248 correlation in regions with pronounced seasons (Fig. 6). The results also show that the correlation for
 249 precipitation is generally larger in tropical regions than in continental regions.



251 Figure 6: Pearson correlation coefficient for different DOY window sizes averaged over the samples for
 252 each Koeppen-Geiger climate zone (A=tropical, B=arid, C=temperate, D=continental).

253 While hourly precipitation can be best reproduced for winter seasons in continental and arid regions,
 254 winter seasons show the lowest correlation for temperate regions. Tropical regions only show
 255 relatively low variations over the year, independently from the selected DOY window size (Fig. 7).
 256 Especially in arid regions, the length of the DOY window size affects the results differently in different
 257 seasons. Here, larger DOY windows decrease the correlation during the rainy season (winter and
 258 spring), while correlation is increased during the dry season (summer and autumn).

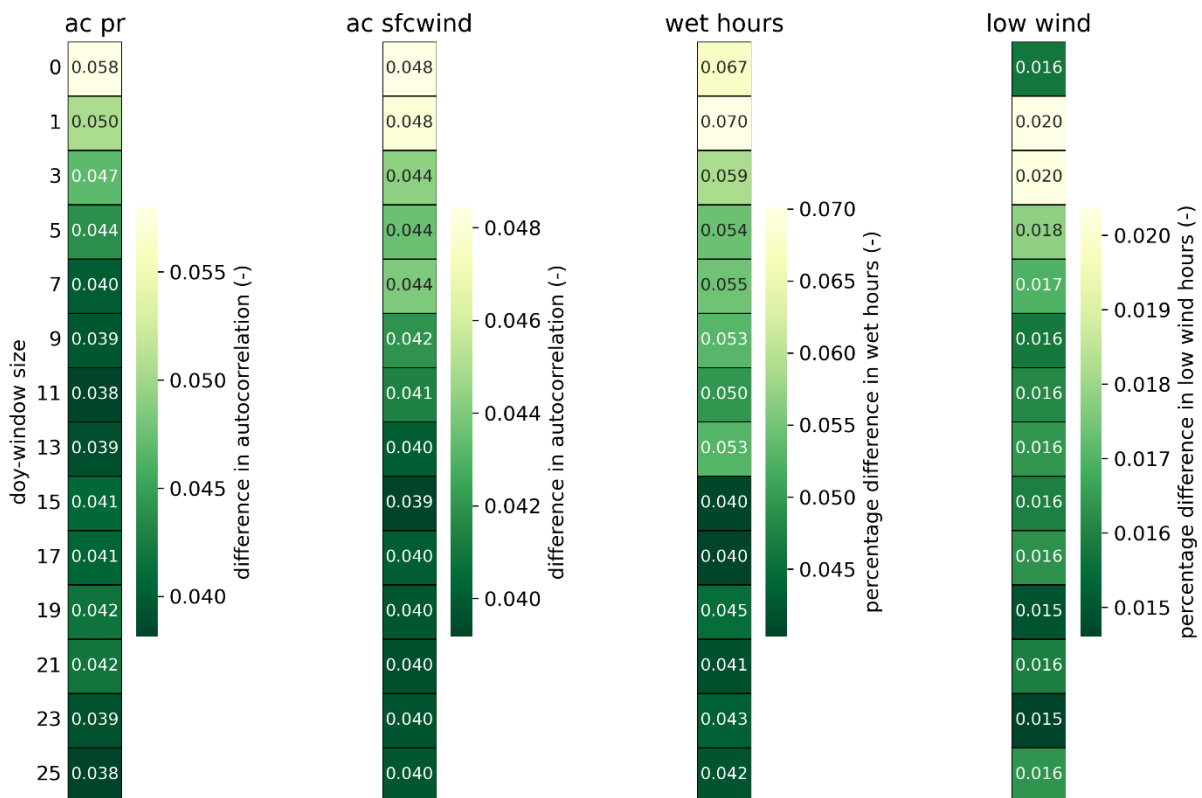


259
 260 Figure 7: Pearson correlation coefficient for different DOY window sizes averaged over the samples for
 261 the four seasons (Northern hemisphere: spring=MAM, summer=JJA, autumn=SON, winter=DJF;
 262 Southern hemisphere: spring=SON, summer=DJF, autumn= MAM, winter=JJA). The heatmap is

263 averaged over the samples for each Koeppen-Geiger climate zone (A=tropical, B=arid, C=temperate,
 264 D=continental).

265 Furthermore, we evaluate the sensitivity of the DOY window size to the reproduction of temporal
 266 autocorrelation (Fig. 8). Therefore, the autocorrelation over lag times between one and 24 hours is
 267 calculated for precipitation and wind speed. Autocorrelation refers to the similarity of a time series to
 268 a lag duration shifted version of the same time series. This allows sub-daily patterns and inter-hour
 269 connectivity to be statistically captured and validated in time series of precipitation and wind speed.
 270 In addition, we also check the reproduction of wet hours (precipitation above 0.1 mm h^{-1}) in 2010 and
 271 the number of hours with low wind speeds (sfcwind $< 2.5 \text{ m s}^{-1}$) referring to the typical cut-in wind
 272 speed of wind turbines.

273 Here, we find that short DOY window sizes below 5 days are not beneficial to all statistics. The
 274 autocorrelation of precipitation (wind speed) is reproduced more accurately with window sizes of 9
 275 days or longer. The number of wet hours is better recreated with window sizes above 15 days. For
 276 hours with low wind speed, a minor improvement is found above 9 days.



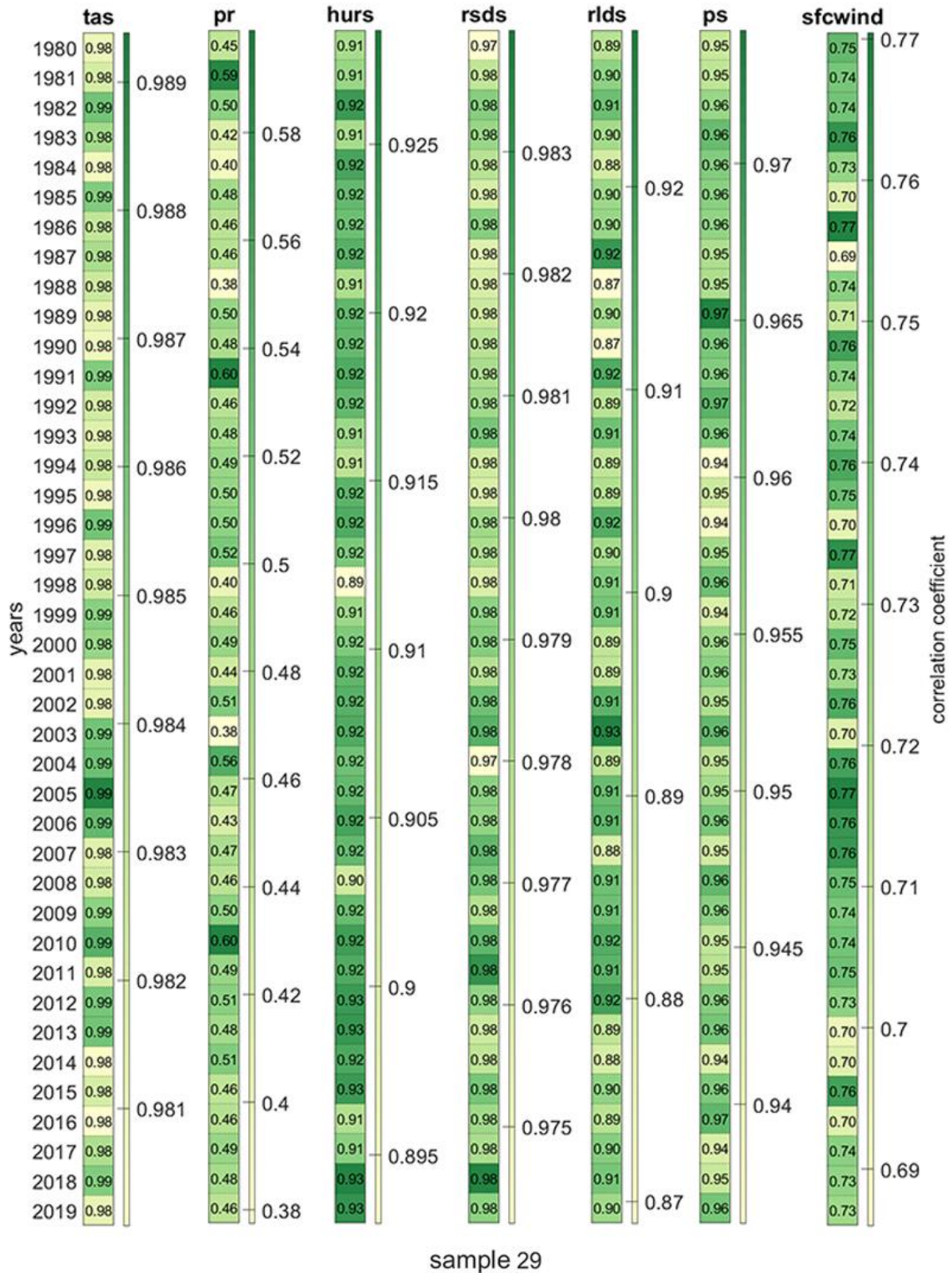
277

278 Figure 8: Extended validation statistics for the sensitivity analysis of the DOY window size for the year
 279 2010. The difference in autocorrelation refers to the average over all 30 samples and lag durations
 280 between one and 24 hours. Wet hours are defined as precipitation intensities above 0.1 mm h^{-1} and
 281 low wind speeds refer to hours with sfcwind $< 2.5 \text{ m s}^{-1}$.

282 4.3 Evaluation of the whole period 1980 – 2019

283 The previous validation has assessed the disaggregation performance for all sample locations for the
 284 year 2010 and different DOY window sizes. For the analysis of the whole time period 1980 – 2019, we
 285 evaluate the 40-year timeseries for sample location 29 and a window size of 11 days. Figure 9 and

286 Supplementary Fig. S5 show the correlation coefficient and mean absolute error, respectively, for each
 287 year to assess the interannual variability of disaggregation performance. For tas, hurs, rsds, rlds, and
 288 ps the performance shows only very minor differences, whereas sfcwind and pr show a higher degree
 289 of interannual fluctuations.



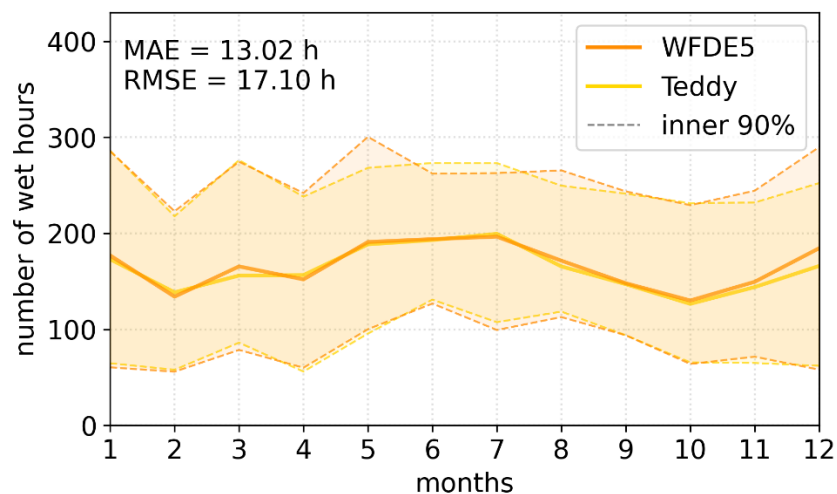
290

291 Figure 9: Pearson correlation coefficient for 1980 – 2019 for sample location 29 and a DOY window
 292 size of 11 days. The scaling of the colorbar differs between variables.

293 4.4 Evaluation of precipitation: Wet proportions and intensities

294 For the further evaluation of precipitation characteristics, also the disaggregated timeseries over the
295 whole period 1980 – 2019 for sample location 29 is assessed. In order to evaluate the reproduction of
296 wet/dry proportions, the monthly cycle of wet hours is provided (Fig. 10). Wet hours above 0.1 mm h^{-1}
297 are recreated by the Teddy-Tool with minor differences for the median over 40 years (Fig. 10). The
298 error measures are calculated for every year separately amounting to a mean absolute error of 13.02
299 h equaling 7.8 %.

300 For the evaluation of the range of precipitation intensities, Fig. 11 shows intensities above 1 mm h^{-1}
301 plotted against its percentage of exceedance for sub-daily durations. We find that the disaggregated
302 precipitation intensities match the original data except for extreme precipitation.

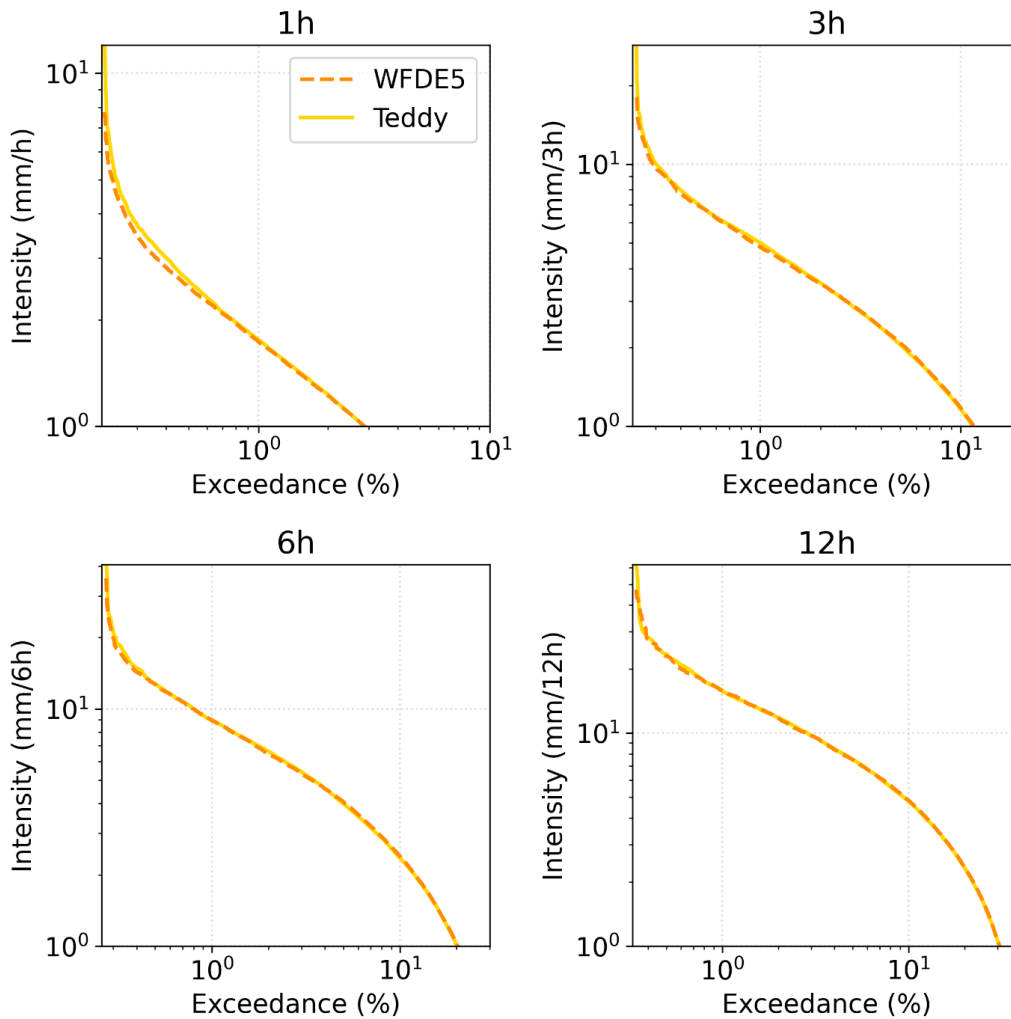


303

304 Figure 10: Number of wet hours per month for sample location 29 in Germany. Solid lines show the
305 median over 40 years, where the dashed lines denote the inner 90% of the 40-year period. MAE and
306 RMSE are calculated separately for every year and averaged over 40 years.

307

308



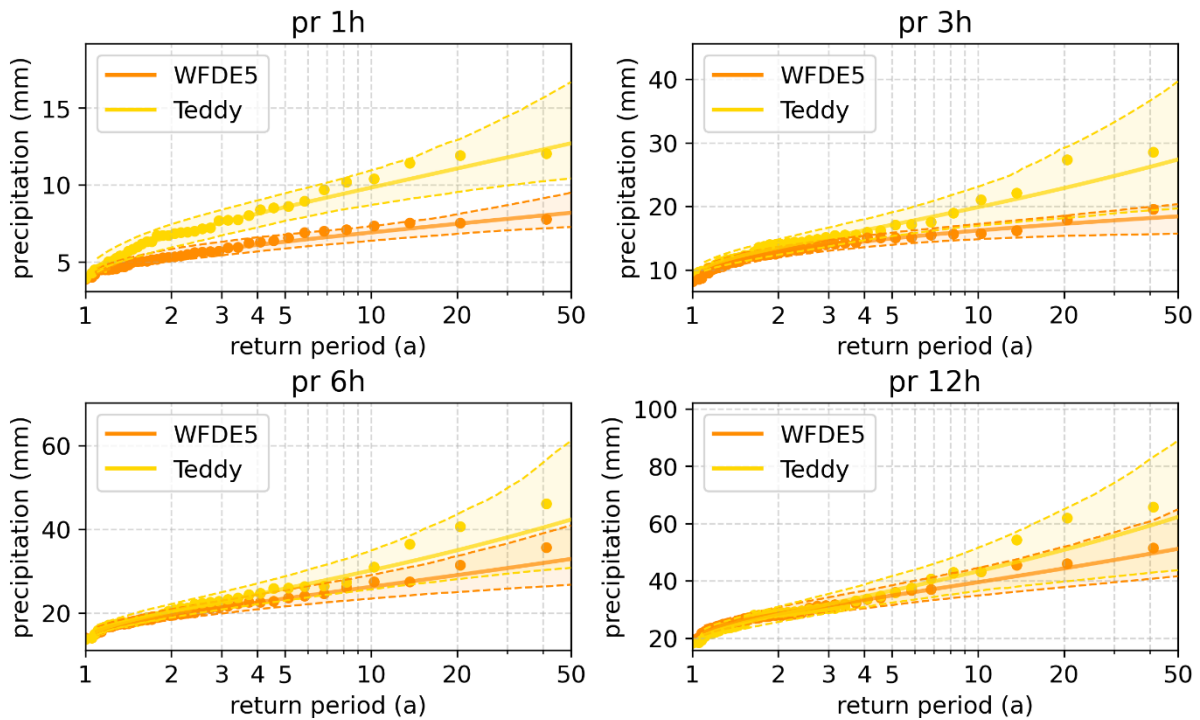
309

310 Figure 11: Exceedance probability of precipitation intensities for sub-daily durations for sample
 311 location 29 in Germany.

312 4.5 Evaluation of precipitation extremes

313 As the ISIMIP data base is used for future impact modelling and historical attribution science (Mengel
 314 et al., 2021), extremes are of major interest for the community. The ability of global climate models to
 315 simulate sub-daily extremes is limited and depends on the variable of interest and the spatio-temporal
 316 conditions of the extreme and the respective model setup (Wehner et al., 2021; Kumar et al., 2015;
 317 Wang and Clow, 2020). However, in this validation, we evaluate how the Teddy-Tool is able to preserve
 318 the statistics of sub-daily extreme values. Therefore, we select precipitation as variable of interest.
 319 Figure 12 shows the reproduction of sub-daily precipitation extremes for 1980 – 2019 for sample
 320 location 29 in southern Germany, where Teddy is run with a DOY window size of 11 days. The 40 annual
 321 maxima are extracted from the original and the disaggregated data. Additionally, the Generalized
 322 Extreme Value (GEV) distribution is fitted to these empirical data. GEV parameters are estimated via
 323 Maximum Likelihood Estimation (Coles, 2001), where the goodness-of-fit is assessed with the
 324 Anderson-Darling test at 95% significance level (Stephens, 1986). Thereby, 95% confidence intervals
 325 are generated applying a bootstrap procedure with 1000 iterations to account for extreme value
 326 statistical uncertainties. We find that the Teddy-Tool leads to an overestimation of annual maximum
 327 precipitation. For the hourly duration, the differences are large with the confidence intervals of the

328 GEV hardly overlapping. For the longer durations, Teddy values approach the original data, with
329 noticeable differences only for the rare events with return periods above 5 years.



330

331 Figure 12: Extreme value statistical evaluation of sub-daily precipitation for sample location 29 in
332 Germany. The annual maxima of the WFDE5 and Teddy are shown as dots. Additionally, GEV fits (lines)
333 with 95% confidence intervals (transparent areas and dashed lines) account for uncertainties. The
334 Teddy-Tool is run with a DOY window size of 11 days.

335 5. Discussion and Outlook

336 The Teddy-Tool allows for temporal disaggregation of daily climate model data. The disaggregation is
337 based on location and time specific empirical relationships between variables. The approach is well
338 suitable for all tested variables and results in very high correlations (>0.9), except for precipitation
339 (>0.5) and wind speed (>0.75). We refer the worse performance for precipitation and wind speed to
340 the high intra-day variability for these variables (Watters et al., 2021). Other variables are governed by
341 a stronger diurnal cycle (Dai and Trenberth, 2004), which is easier to disaggregate based on empirical
342 diurnal profiles.

343 Compared to other approaches, the advantage of the Teddy-Tool is that no other input data is required
344 rather than the daily climate model data. The Teddy-Tool is relatively simple to apply, considers specific
345 local and seasonal features of the diurnal course of different climate variables, and preserves the
346 physical consistency of inter-variable relationships. Mass and energy are conserved and mean daily
347 values of the climate model are reproduced any time.

348 The spatial and temporal resolution of the results is determined by the provided temporal and spatial
349 resolution of the chosen reference data (WFDE5 used here). Longer available reanalysis time periods
350 extend the statistical population for identifying the most similar weather conditions in the past and
351 thus could improve the results. Generally, also other reference data could be used, that provides higher
352 temporal or spatial resolution for a specific region.

353 The DOY window to find the most similar historical weather situations can be chosen in different sizes.
354 For most of the variables, we found small effects of time window adjustments, except for precipitation
355 and wind speed. The evaluation of different DOY window sizes reveals that a DOY window size of 11
356 can generally be recommended across all variables. Larger DOY windows should be avoided mainly in
357 arid regions, while shorter DOY windows generally lead to poorer representations of autocorrelation
358 and extreme events.

359 One limitation of the Teddy-Tool is the representation of extreme events, mainly for precipitation,
360 which is generally the most difficult variable for temporal disaggregation. We found that hourly
361 precipitation extremes are overestimated. For heavy daily precipitation events, Teddy distributes the
362 24h-sums either correctly, too evenly or on too few hours. When distributing on too few hours,
363 extreme hourly intensities evolve, which may have never occurred or may even be physically
364 implausible. For temporal disaggregation of extreme precipitation, we recommend dynamical
365 downscaling via high-resolution climate models (Poschlod, 2021; Poschlod et al., 2021; Zabel et al.,
366 2012; Zabel and Mauser, 2013).

367 Another limitation of the approach is the reproduction of the inter-day connectivity within the
368 disaggregated time series. When two diurnal profiles are chosen for the disaggregation of adjacent
369 days, which show dissimilar courses in the time steps at the change of the day, abrupt value jumps
370 might occur in the disaggregation. This can be seen in Fig. 3 for rlds from July 4th to July 5th. To illustrate
371 this issue, a disaggregation time series from another location is provided in Supplementary Fig. S2. This
372 limitation does also apply for the Method of Fragments applied on precipitation (Li et al., 2018).
373 Similarly to Li et al. (2018), we also consider the precipitation state of the previous and following day
374 to improve inter-day connectivity. Without this additional consideration, overnight precipitation
375 events would often be 'cut off' in the disaggregation. For the remaining abrupt jumps in the
376 disaggregated time series, we refrain from post-processing with subsequent smoothing, as we want to
377 preserve both mass and energy and the empirical diurnal profiles.

378 For the disaggregation of future climate projections using of the Teddy-Tool, we have the following
379 remarks: As the Teddy-Tool derives the relationships between sub-daily and daily values empirically
380 based on reanalysis data, future diurnal profiles, which are outside the historical range of diurnal
381 profiles, might possibly be not fully reproduced. However, this limitation is common for statistical
382 approaches, which are to be calibrated on historical data (Papalexiou et al., 2018). Nevertheless, due
383 to energy and mass conservation, climate trends in the daily climate signal are fully preserved. Hence,
384 applying Teddy for temporal disaggregation under climate change holds under the assumption that we
385 select the most similar meteorological day of the historical data and that this diurnal profile is
386 representative for future climatic conditions. However, this assumption might apply to a different
387 degree for different variables. We expect non-stationarity for the diurnal profiles due to changing
388 weather patterns, shifts in rainfall generating processes, and shifts in the seasonality, mainly for
389 precipitation and wind. The daily course of other variables, such as solar radiation and temperature
390 might generally be less affected by a warmer climate. Furthermore, global climate models at coarse
391 resolutions generally do not represent all processes to fully reproduce intra-day variability. Teddy
392 applies the diurnal profiles and intra-day variability from the WFDE5 data, which are bias-adjusted
393 ERA5 reanalysis data that implicitly consider finer scale effects than coarse-resolution global climate
394 models (Cucchi et al., 2020). Thus, the disaggregation process in Teddy is consistent with the bias
395 adjustment in ISIMIP3.

396 Another limitation of the methodology could occur in the case of strong climate change signals. In case
397 of high warming in end-of-century projections, the number of sampled historical days might decrease
398 if the same historical day is sampled repeatedly. This could lead to reductions in diversity of the diurnal
399 profile. Hence, Teddy allows to monitor the number of unique analogue days per year. An additional
400 analysis for SSP3-7.0 using the GFDL-ESM4 climate model shows that the number of unique analogue
401 climate days are declining, as expected, but still the diversity of chosen days is above 300 unique days
402 at the end of the century for a chosen moving-window size of ± 11 days (Supplementary Fig. S6). A
403 smaller size of the moving window prevents that the same analogue day is chosen over a longer time
404 period. This will increase the diversity of diurnal profiles at the expense of similarity. Even if diurnal
405 profiles are derived from the same analogue day repeatedly, the disaggregated diurnal courses, e.g.
406 for temperature, will show variations (different offset and different amplitude) due to conservation of
407 daily mean energy and mass. From a broader perspective, it is also not clear whether the uncertainties
408 resulting from this limitation are larger than the uncertainties within the climate model projections
409 until the end of the century. Furthermore, in the long term, the basic population for finding analogue
410 climates will continuously increase, since WFDE5 data, which are based on ERA5, are continuously
411 updated. We note that Teddy could be also employed to disaggregate future daily climate projections
412 based on hourly future climate projections as reference.

413 Further possible developments could include improvements for the reproduction of the inter-day
414 connectivity. Despite the consideration of precipitation classes, still abrupt value jumps over day
415 changes are possible. A future introduction of temperature classes and surface pressure classes in
416 addition to the precipitation classes could help to reduce this effect. Depending on the location of
417 interest, also including climate modes or weather patterns for the choice of the most similar
418 meteorological day could positively affect the performance. Furthermore, depending on the
419 application, it could be reasonable not to screen for the most similar meteorological day, but for the
420 most similar succession of multiple days. This would as a consequence improve the inter-day
421 connectivity as less different profiles are selected.

422 Other optional future developments could include the separation of direct and diffuse radiation, which
423 is also a required information for some impact models which is currently not provided by ISIMIP.
424 However, we would make further development with more options dependent on the community's
425 adoption of the current executable tool.

426 **Code availability**

427 The source code of the Teddy-Tool (v1.1) and a parallelized version of the Teddy-Tool (v1.1p), including
428 a precompiled executable file for Windows, preprocessed data, results of the cross-validation and
429 exemplary results for SSP 585 (2015 – 2100) and the UKESM1-0-L climate model for 30 samples are
430 provided via Zenodo (<https://doi.org/10.5281/zenodo.8124111>).

431 **Author contribution**

432 FZ: Conceptualization, Software, Methodology, Validation, Formal analysis, Resources, Data curation,
433 Writing - original draft, Visualization

434 BP: Methodology, Validation, Formal analysis, Writing - original draft, Visualization

435 **Competing interests**

436 The contact author has declared that none of the authors has any competing interests.

437 **Acknowledgements**

438 We acknowledge the methodological discussion with Stefan Lange from the Potsdam Institute of
439 Climate Impact Research (PIK).

440 **References**

- 441 Ailliot, P., Allard, D., Monbet, V., and Naveau, P.: Stochastic weather generators: an overview of
442 weather type models, *Journal de la société française de statistique*, 156, <https://doi.org/101-113>,
443 2015.
- 444 Beck, H. E., Zimmermann, N. E., McVicar, T. R., Vergopolan, N., Berg, A., and Wood, E. F.: Present and
445 future Köppen-Geiger climate classification maps at 1-km resolution, *Scientific Data*, 5, 180214,
446 <https://doi.org/10.1038/sdata.2018.214>, 2018.
- 447 Bennett, A., Hamman, J. & Nijssen, B.: MetSim: A python package for estimation and disaggregation
448 of meteorological data, *Journal of Open Source Software*, 5(47), 2042,
449 <https://doi.org/10.21105/joss.02042>, 2020.
- 450 Breinl, K. and Di Baldassarre, G.: Space-time disaggregation of precipitation and temperature across
451 different climates and spatial scales, *Journal of Hydrology: Regional Studies*, 21, 126-146,
452 <https://doi.org/10.1016/j.ejrh.2018.12.002>, 2019.
- 453 Buck, A. L.: New Equations for Computing Vapor Pressure and Enhancement Factor, *Journal of*
454 *Applied Meteorology and Climatology*, 20, 1527-1532, [https://doi.org/10.1175/1520-0450\(1981\)020<1527:Nefcvp>2.0.Co;2](https://doi.org/10.1175/1520-0450(1981)020<1527:Nefcvp>2.0.Co;2), 1981.
- 456 Byers, E., Gidden, M., Leclère, D., Balkovic, J., Burek, P., Ebi, K., Greve, P., Grey, D., Havlik, P., Hillers,
457 A., Johnson, N., Kahil, T., Krey, V., Langan, S., Nakicenovic, N., Novak, R., Obersteiner, M.,
458 Pachauri, S., Palazzo, A., Parkinson, S., Rao, N. D., Rogelj, J., Satoh, Y., Wada, Y., Willaarts, B., and
459 Riahi, K.: Global exposure and vulnerability to multi-sector development and climate change
460 hotspots, *Environmental Research Letters*, 13, 055012, <https://doi.org/10.1088/1748-9326/aabf45>, 2018.
- 462 Chen, D., Dai, A., and Hall, A.: The Convective-To-Total Precipitation Ratio and the “Drizzling” Bias in
463 Climate Models, *Journal of Geophysical Research: Atmospheres*, 126, e2020JD034198,
464 <https://doi.org/10.1029/2020JD034198>, 2021.
- 465 Chen, C. J.: Temporal disaggregation of seasonal forecasting for streamflow simulation. *World*
466 *Environmental and Water Resources Congress 2016*, pp. 63-72, 2016.
- 467 Coles, S.: *An Introduction to Statistical Modeling of Extreme Values*. Springer, London, U.K.
468 <https://doi.org/10.1007/978-1-4471-3675-0>, 2001.
- 469 Colón-González, F. J., Sewe, M. O., Tompkins, A. M., Sjödin, H., Casallas, A., Rocklöv, J., Caminade, C.,
470 and Lowe, R.: Projecting the risk of mosquito-borne diseases in a warmer and more populated
471 world: a multi-model, multi-scenario intercomparison modelling study, *The Lancet Planetary*
472 *Health*, 5, e404-e414, [https://doi.org/10.1016/S2542-5196\(21\)00132-7](https://doi.org/10.1016/S2542-5196(21)00132-7), 2021.
- 473 Cucchi, M., Weedon, G. P., Amici, A., Bellouin, N., Lange, S., Müller Schmied, H., Hersbach, H., and
474 Buontempo, C.: WFDE5: bias-adjusted ERA5 reanalysis data for impact studies, *Earth Syst. Sci.*
475 *Data*, 12, 2097-2120, <https://doi.org/10.5194/essd-12-2097-2020>, 2020.
- 476 Dai, A. and Trenberth, K. E.: The Diurnal Cycle and Its Depiction in the Community Climate System
477 Model. *Journal of Climate*, 17, 930-951, [https://doi.org/10.1175/1520-0442\(2004\)017<0930:TDCAID>2.0.CO;2](https://doi.org/10.1175/1520-0442(2004)017<0930:TDCAID>2.0.CO;2), 2004.
- 479 Debele, B., Srinivasan, R., and Yves Parlange, J.: Accuracy evaluation of weather data generation and
480 disaggregation methods at finer timescales, *Advances in Water Resources*, 30, 1286-1300,
481 <https://doi.org/10.1016/j.advwatres.2006.11.009>, 2007.
- 482 Degife, A. W., Zabel, F., and Mauser, W.: Climate change impacts on potential maize yields in
483 Gambella region, Ethiopia, *Regional Environmental Change*, <https://doi.org/10.1007/s10113-021-01773-3>, 2021.

485 Eyring, V., Bony, S., Meehl, G. A., Senior, C. A., Stevens, B., Stouffer, R. J., and Taylor, K. E.: Overview
486 of the Coupled Model Intercomparison Project Phase 6 (CMIP6) experimental design and
487 organization, *Geosci. Model Dev.*, 9, 1937-1958, <https://doi.org/10.5194/gmd-9-1937-2016>, 2016.

488 Förster, K., Hanzer, F., Winter, B., Marke, T., and Strasser, U.: An open-source MEteoroLOGical
489 observation time series DISaggregation Tool (MELODIST v0.1.1), *Geosci. Model Dev.*, 9, 2315-
490 2333, <https://doi.org/10.5194/gmd-9-2315-2016>, 2016.

491 Franke, J. A., Müller, C., Minoli, S., Elliott, J., Folberth, C., Gardner, C., Hank, T., Izaurrealde, R. C.,
492 Jägermeyr, J., Jones, C. D., Liu, W., Olin, S., Pugh, T. A. M., Ruane, A. C., Stephens, H., Zabel, F., and
493 Moyer, E. J.: Agricultural breadbaskets shift poleward given adaptive farmer behavior under
494 climate change, *Global Change Biol*, 28, 167-181, <https://doi.org/10.1111/gcb.15868>, 2022.

495 Golub, M., Thiery, W., Marcé, R., Pierson, D., Vanderkelen, I., Mercado-Bettin, D., Woolway, R. I.,
496 Grant, L., Jennings, E., Kraemer, B. M., Schewe, J., Zhao, F., Frieler, K., Mengel, M., Bogomolov, V.
497 Y., Bouffard, D., Côté, M., Couture, R. M., Debolskiy, A. V., Droppers, B., Gal, G., Guo, M., Janssen,
498 A. B. G., Kirillin, G., Ladwig, R., Magee, M., Moore, T., Perroud, M., Piccolroaz, S., Raaman Vinnaa,
499 L., Schmid, M., Shatwell, T., Stepanenko, V. M., Tan, Z., Woodward, B., Yao, H., Adrian, R., Allan,
500 M., Anneville, O., Arvola, L., Atkins, K., Boegman, L., Carey, C., Christianson, K., de Eyto, E.,
501 DeGasperi, C., Grechushnikova, M., Hejzlar, J., Joehnk, K., Jones, I. D., Laas, A., Mackay, E. B.,
502 Mammarella, I., Markensten, H., McBride, C., Özkundakci, D., Potes, M., Rinke, K., Robertson, D.,
503 Rusak, J. A., Salgado, R., van der Linden, L., Verburg, P., Wain, D., Ward, N. K., Wollrab, S., and
504 Zdorovenova, G.: A framework for ensemble modelling of climate change impacts on lakes
505 worldwide: the ISIMIP Lake Sector, *Geosci. Model Dev.*, 15, <https://doi.org/4597-4623>,
506 10.5194/gmd-15-4597-2022, 2022.

507 Görner, C., Franke, J., Kronenberg, R., Hellmuth, O., and Bernhofer, C.: Multivariate non-parametric
508 Euclidean distance model for hourly disaggregation of daily climate data, *Theoretical and Applied
509 Climatology*, 143, 241-265, <https://doi.org/10.1007/s00704-020-03426-7>, 2021.

510 Jägermeyr, J., Müller, C., Ruane, A. C., Elliott, J., Balkovic, J., Castillo, O., Faye, B., Foster, I., Folberth,
511 C., Franke, J. A., Fuchs, K., Guarin, J. R., Heinke, J., Hoogenboom, G., Iizumi, T., Jain, A. K., Kelly, D.,
512 Khabarov, N., Lange, S., Lin, T.-S., Liu, W., Mialyk, O., Minoli, S., Moyer, E. J., Okada, M., Phillips,
513 M., Porter, C., Rabin, S. S., Scheer, C., Schneider, J. M., Schyns, J. F., Skalsky, R., Smerald, A., Stella,
514 T., Stephens, H., Webber, H., Zabel, F., and Rosenzweig, C.: Climate impacts on global agriculture
515 emerge earlier in new generation of climate and crop models, *Nature Food*, 2, 873-885,
516 <https://doi.org/10.1038/s43016-021-00400-y>, 2021.

517 Jukes, M., Taylor, K. E., Durack, P. J., Lawrence, B., Mizielinski, M. S., Pamment, A., Peterschmitt, J.-
518 Y., Rixen, M., and Sényi, S.: The CMIP6 Data Request (DREQ, version 01.00.31), *Geosci. Model
519 Dev.*, 13, 201-224, <https://doi.org/10.5194/gmd-13-201-2020>, 2020.

520 Kumar, D., Mishra, V., and Ganguly, A. R.: Evaluating wind extremes in CMIP5 climate models,
521 *Climate Dynamics*, 45, 441-453, <https://doi.org/10.1007/s00382-014-2306-2>, 2015.

522 Kunstmann, H. and Stadler, C.: High resolution distributed atmospheric-hydrological modelling for
523 Alpine catchments, *Journal of Hydrology*, 314, 105-124,
524 <https://doi.org/10.1016/j.jhydrol.2005.03.033>, 2005.

525 Lange, S.: Trend-preserving bias adjustment and statistical downscaling with ISIMIP3BASD (v1.0),
526 *Geosci. Model Dev.*, 12, 3055-3070, <https://doi.org/10.5194/gmd-12-3055-2019>, 2019.

527 Li, X., Meshgi, A., Wang, X., Zhang, J., Tay, S. H. X., Pijcke, G., Manocha, N., Ong, M., Nguyen, M. T.,
528 and Babovic, V.: Three resampling approaches based on method of fragments for daily-to-subdaily
529 precipitation disaggregation, *International Journal of Climatology*, 38, e1119-e1138,
530 <https://doi.org/10.1002/joc.5438>, 2018.

531 Liston, G. E. and Elder, K.: A Meteorological Distribution System for High-Resolution Terrestrial
532 Modeling (MicroMet), *Journal of Hydrometeorology*, 7, 217-234,
533 <https://doi.org/10.1175/jhm486.1>, 2006.

534 Liu, C., Ikeda, K., Thompson, G., Rasmussen, R., and Dudhia, J.: High-Resolution Simulations of
535 Wintertime Precipitation in the Colorado Headwaters Region: Sensitivity to Physics

536 Parameterizations, *Monthly Weather Review*, 139, 3533-3553, [https://doi.org/10.1175/MWR-D-](https://doi.org/10.1175/MWR-D-11-00009.1)
537 11-00009.1, 2011.

538 Lüttgau, J., Kunkel, J.: Cost and Performance Modeling for Earth System Data Management and
539 Beyond. In: Yokota, R., Weiland, M., Shalf, J., Alam, S. (eds) *High Performance Computing. ISC High*
540 *Performance 2018. Lecture Notes in Computer Science*, vol 11203. Springer, Cham.
541 https://doi.org/10.1007/978-3-030-02465-9_2, 2018.

542 Mengel, M., Treu, S., Lange, S., and Frieler, K.: ATTRICI v1.1 – counterfactual climate for impact
543 attribution, *Geosci. Model Dev.*, 14, 5269-5284, <https://doi.org/10.5194/gmd-14-5269-2021>,
544 2021.

545 Meredith, E., Ulbrich, U., Rust, H. W., and Truhetz, H.: Present and future diurnal hourly precipitation
546 in 0.11° EURO-CORDEX models and at convection-permitting resolution, *Environmental Research*
547 *Communications*, 3, 055002, <https://doi.org/10.1088/2515-7620/abf15e>, 2021.

548 Mezghani, A. and Hingray, B.: A combined downscaling-disaggregation weather generator for
549 stochastic generation of multisite hourly weather variables over complex terrain: Development
550 and multi-scale validation for the Upper Rhone River basin, *Journal of Hydrology*, 377, 245-260,
551 <https://doi.org/10.1016/j.jhydrol.2009.08.033>, 2009.

552 Minoli, S., Jägermeyr, J., Asseng, S., Urfels, A., and Müller, C.: Global crop yields can be lifted by
553 timely adaptation of growing periods to climate change, *Nature Communications*, 13, 7079,
554 <https://doi.org/10.1038/s41467-022-34411-5>, 2022.

555 Orlov, A., Daloz, A. S., Sillmann, J., Thiery, W., Douzal, C., Lejeune, Q., and Schleussner, C.: Global
556 Economic Responses to Heat Stress Impacts on Worker Productivity in Crop Production,
557 *Economics of Disasters and Climate Change*, 5, 367-390, [https://doi.org/10.1007/s41885-021-](https://doi.org/10.1007/s41885-021-00091-6)
558 00091-6, 2021.

559 Orlov, A., et al.: Human heat stress could offset economic benefits of the CO2 fertilisation effect in
560 crop production. *Nature Communications: Under Review*, 2023.

561 Papalexiou, S. M., Markonis, Y., Lombardo, F., AghaKouchak, A., and Foufoula-Georgiou, E.: Precise
562 Temporal Disaggregation Preserving Marginals and Correlations (DiPMaC) for Stationary and
563 Nonstationary Processes, *Water Resources Research*, 54, 7435-7458,
564 <https://doi.org/10.1029/2018WR022726>, 2018.

565 Park, H. and Chung, G.: A Nonparametric Stochastic Approach for Disaggregation of Daily to Hourly
566 Rainfall Using 3-Day Rainfall Patterns, *Water*, 12, 2306, 2020.

567 Portmann, F. T., Siebert, S., and Döll, P.: MIRCA2000—Global monthly irrigated and rainfed crop
568 areas around the year 2000: A new high-resolution data set for agricultural and hydrological
569 modeling, *Global Biogeochemical Cycles*, 24, <https://doi.org/10.1029/2008GB003435>, 2010.

570 Poschlod, B.: Using high-resolution regional climate models to estimate return levels of daily extreme
571 precipitation over Bavaria, *Nat. Hazards Earth Syst. Sci.*, 21, 3573-3598,
572 <https://doi.org/10.5194/nhess-21-3573-2021>, 2021.

573 Poschlod, B.: Attributing heavy rainfall event in Berchtesgadener Land to recent climate change –
574 Further rainfall intensification projected for the future, *Weather Clim Extremes*, 38, 100492,
575 <https://doi.org/10.1016/j.wace.2022.100492>, 2022.

576 Poschlod, B. and Ludwig, R.: Internal variability and temperature scaling of future sub-daily rainfall
577 return levels over Europe, *Environmental Research Letters*, 16, 064097,
578 <https://doi.org/10.1088/1748-9326/ac0849>, 2021.

579 Poschlod, B., Ludwig, R., and Sillmann, J.: Ten-year return levels of sub-daily extreme precipitation
580 over Europe, *Earth Syst. Sci. Data*, 13, 983-1003, <https://doi.org/10.5194/essd-13-983-2021>, 2021.

581 Poschlod, B., Hodnebrog, Ø., Wood, R. R., Alterskjær, K., Ludwig, R., Myhre, G., and Sillmann, J.:
582 Comparison and Evaluation of Statistical Rainfall Disaggregation and High-Resolution Dynamical
583 Downscaling over Complex Terrain, *Journal of Hydrometeorology*, 19, 1973-1982,
584 <https://doi.org/10.1175/jhm-d-18-0132.1>, 2018.

585 Pui, A., Sharma, A., Mehrotra, R., Sivakumar, B., and Jeremiah, E.: A comparison of alternatives for
586 daily to sub-daily rainfall disaggregation, *J. Hydrol.*, 470, 138– 157,
587 <https://doi.org/10.1016/j.jhydrol.2012.08.041>, 2012.

588 Reed, C., Anderson, W., Kruczkiewicz, A., Nakamura, J., Gallo, D., Seager, R., and McDermid, S. S.: The
589 impact of flooding on food security across Africa, *Proceedings of the National Academy of*
590 *Sciences*, 119, e2119399119, <https://doi.org/10.1073/pnas.2119399119>, 2022.

591 Sharma, A. and Srikanthan, S.: Continuous Rainfall Simulation: A Nonparametric Alternative, in:
592 30th Hydrology & Water Resources Symposium: Past, Present & Future, 4–7 December 2006,
593 Launceston, Tasmania, p. 86, 2006.

594 Stephens, A. M.: Tests based on EDF statistics. In: D’Agostino, R. B. and Stephens, M. A. (eds.):
595 Goodness-of-fit techniques, 1986.

596 Sun, Y., Solomon, S., Dai, A., and Portmann, R. W.: How Often Does It Rain?, *Journal of Climate*, 19,
597 <https://doi.org/916-934>, 10.1175/jcli3672.1, 2006.

598 Tittensor, D. P., Novaglio, C., Harrison, C. S., Heneghan, R. F., Barrier, N., Bianchi, D., Bopp, L.,
599 Bryndum-Buchholz, A., Britten, G. L., Büchner, M., Cheung, W. W. L., Christensen, V., Coll, M.,
600 Dunne, J. P., Eddy, T. D., Everett, J. D., Fernandes-Salvador, J. A., Fulton, E. A., Galbraith, E. D.,
601 Gascuel, D., Guiet, J., John, J. G., Link, J. S., Lotze, H. K., Maury, O., Ortega-Cisneros, K., Palacios-
602 Abrantes, J., Petrik, C. M., du Pontavice, H., Rault, J., Richardson, A. J., Shannon, L., Shin, Y.-J.,
603 Steenbeek, J., Stock, C. A., and Blanchard, J. L.: Next-generation ensemble projections reveal
604 higher climate risks for marine ecosystems, *Nat Clim Change*, 11, 973-981,
605 <https://doi.org/10.1038/s41558-021-01173-9>, 2021.

606 Trinanes, J. and Martinez-Urtaza, J.: Future scenarios of risk of *Vibrio* infections in a warming planet:
607 a global mapping study, *The Lancet Planetary Health*, 5, e426-e435,
608 [https://doi.org/10.1016/S2542-5196\(21\)00169-8](https://doi.org/10.1016/S2542-5196(21)00169-8), 2021.

609 Verfaillie, D., Déqué, M., Morin, S., and Lafaysse, M.: The method ADAMONT v1.0 for statistical
610 adjustment of climate projections applicable to energy balance land surface models, *Geosci.*
611 *Model Dev.*, 10, 4257-4283, <https://doi.org/10.5194/gmd-10-4257-2017>, 2017.

612 Vormoor, K. and Skaugen, T.: Temporal Disaggregation of Daily Temperature and Precipitation Grid
613 Data for Norway, *Journal of Hydrometeorology*, 14, 989-999, [https://doi.org/10.1175/jhm-d-12-](https://doi.org/10.1175/jhm-d-12-0139.1)
614 0139.1, 2013.

615 Wang, K. and Clow, G. D.: The Diurnal Temperature Range in CMIP6 Models: Climatology, Variability,
616 and Evolution, *Journal of Climate*, 33, 8261-8279, <https://doi.org/10.1175/jcli-d-19-0897.1>, 2020.

617 Warszawski, L., Frieler, K., Huber, V., Piontek, F., Serdeczny, O., and Schewe, J.: The Inter-Sectoral
618 Impact Model Intercomparison Project (ISI-MIP): Project framework, *Proceedings of the National*
619 *Academy of Sciences*, 111, 3228-3232, <https://doi.org/10.1073/pnas.1312330110>, 2014.

620 Watters, D., Battaglia, A., and Allan, R.: The Diurnal Cycle of Precipitation according to Multiple
621 Decades of Global Satellite Observations, Three CMIP6 Models, and the ECMWF Reanalysis,
622 *Journal of Climate*, 34, 5063-5080, <https://doi.org/10.1175/JCLI-D-20-0966.1>, 2021.

623 Wehner, M., Lee, J., Risser, M., Ullrich, P., Gleckler, P., and Collins, W. D.: Evaluation of extreme sub-
624 daily precipitation in high-resolution global climate model simulations, *Philosophical Transactions*
625 *of the Royal Society A: Mathematical, Physical and Engineering Sciences*, 379, 20190545,
626 <https://doi.org/10.1098/rsta.2019.0545>, 2021.

627 Zabel, F. and Mauser, W.: 2-way coupling the hydrological land surface model PROMET with the
628 regional climate model MM5, *Hydrology and Earth System Sciences*, 17, 1705–1714,
629 <https://doi.org/10.5194/hess-17-1705-2013>, 2013.

630 Zabel, F., Mauser, W., Marke, T., Pfeiffer, A., Zängl, G., and Wastl, C.: Inter-comparison of two land-
631 surface models applied at different scales and their feedbacks while coupled with a regional
632 climate model, *Hydrology and Earth System Sciences*, 16, 1017–1031,
633 <https://doi.org/10.5194/hess-16-1017-2012>, 2012.

634 Zabel, F., Müller, C., Elliott, J., Minoli, S., Jägermeyr, J., Schneider, J. M., Franke, J. A., Moyer, E., Dury,
635 M., Francois, L., Folberth, C., Liu, W., Pugh, T. A. M., Olin, S., Rabin, S. S., Mauser, W., Hank, T.,
636 Ruane, A. C., and Asseng, S.: Large potential for crop production adaptation depends on available
637 future varieties, *Global Change Biol*, 27, 3870-3882 <https://doi.org/10.1111/gcb.15649>, 2021.

638 Zhao, W., Kinouchi, T., and Nguyen, H. Q.: A framework for projecting future intensity-duration-
639 frequency (IDF) curves based on CORDEX Southeast Asia multi-model simulations: An application

640 for two cities in Southern Vietnam, Journal of Hydrology, 598, 126461,
641 <https://doi.org/10.1016/j.jhydrol.2021.126461>, 2021.